

Article citation info:

Chen Q, Wang J, Integrated Multi-Energy Hub Optimization: A Model for Reliable, Economically Efficient, and Sustainable Energy Systems, *Eksploracja i Niezawodność – Maintenance and Reliability* 2025: 27(3) <http://doi.org/10.17531/ein/201335>

Integrated Multi-Energy Hub Optimization: A Model for Reliable, Economically Efficient, and Sustainable Energy Systems

Indexed by:
 Web of Science Group

Qiuju Chen^a, Jungang Wang^{b,*}

^a School of Economics and Management, Qujing Normal University, China

^b Shandong Changzhi Construction Engineering Co., LTD, China

Highlights


- Integrating renewables, CHP, P2G, and hydrogen storage in a multi-objective model.
- Addressing supply-demand uncertainties to sustainable & reliable capacity planning.
- Enhancing optimization precision, robustness, and speed with the PSO-GOA algorithm.
- Ensuring uninterrupted energy supply despite renewable energy source variability.
- Converting surplus renewables to hydrogen for use during energy-deficient periods.

Abstract

The presented assessment provides a multi-objective optimization framework for independent multi-energy hubs, which integrates electricity, heat, and hydrogen systems. A hybridization of particle swarm and grasshopper optimization algorithms is utilized to handle renewable energy uncertainties and ensure high reliability, economic efficiency, and renewable energy utilization. A powerful capacity configuration strategy balances economic and environmental purposes while elevating system reliability. Hydrogen storage and methanation minimize renewable energy curtailment and improve flexibility. Stochastic optimization with scenario generation and reduction effectively models uncertainties. Besides, advanced coordination of renewable sources, cooling, heating, power units, and storage systems guarantees efficient dispatch. Hydrogen-to-methane conversion and gas boilers improved adaptability. Validation through three case studies depicts a 99.8% REU rate, only 32 kWh of unsupplied energy, and an optimized cost of \$3,889.50, which confirms the framework's efficacy for complex energy scenarios.

Keywords

multi-energy hubs, renewable energy integration, stochastic optimization, hybrid PSO-GOA algorithm, hydrogen storage systems

This is an open access article under the CC BY license (<https://creativecommons.org/licenses/by/4.0/>) 

1. Introduction

In response to intensifying global concerns regarding the depletion of fossil fuel reserves and the escalating global energy demand, the pursuit of clean and sustainable energy sources has gained significant momentum [1]. This shift is motivated by the urgent need to address environmental challenges, enhance energy security, and promote economic growth through the adoption of renewable energy technologies [2]. The evolution of energy systems has highlighted the critical role of integrating diverse renewable energy sources, such as wind, solar, and hydrogen, into

scalable and efficient energy infrastructure [3].

According to these aspects, the opportunity can be considered to be important. The idea here is that MEHs represent an enabling framework for the achievement of reliable and sustainable energy systems. MEH represents a new paradigm in decentralized energy supply and distribution toward higher levels of local energy self-sufficiency and better efficiency in renewable resources management. They can handle multiple energy vectors, including electricity, heat, and hydrogen, and are thus put in

(*) Corresponding author.

E-mail addresses:

Q. Chen, (0009-0004-8526-3519) chenqiuju@mail.qjnu.edu.cn, J. Wang (ORCID: 0009-0002-3125-4559) 708875688@qq.com,

a place of prominence as facilitators toward the full exploitation of renewable energy sources. Moreover, it addresses problems of intermittence and variability of the output of renewable energy conversion, hence ensuring a reliable and secure energy supply [4].

The future trend of worldwide energy systems calls for the different disseminated independent energy nodes that are meant to work optimally under technical, economic, and environmental constraints [5]. The different design processes and their actual deployment from scratch are very complex in nature and pose a lot of technical and logistical challenges. This complexity is further exacerbated by the need to meet a wide range of different energy requirements, together with the goal of achieving maximum renewable energy integration, given highly uncertain operational conditions [6]. The role of MEHs goes beyond energy provision to include energy flow optimization, operational cost reduction, and environmental impact minimization. While prior studies have made significant strides in exploring capacity configurations for MEHs, most have focused on single-objective functions, limiting their applicability to broader configuration requirements [7]. For instance, optimal MEH planning in Beijing's Haidian District demonstrated superior economic and environmental performance compared to traditional centralized systems. Similarly, studies in Greek residential areas highlighted cost-saving potential but often neglected supply stability, underlining the need for more comprehensive approaches [8].

Recent research has underscored the importance of addressing uncertainties inherent in renewable energy sources, such as solar radiation variability and wind speed fluctuations. Advanced methods like stochastic and robust optimization have been employed to tackle these challenges, but they often result in overly conservative designs with limited economic feasibility [9]. Moreover, emerging technologies like power-to-gas (P2G) and hydrogen energy storage offer promising solutions for enhancing REU, yet their integration into MEHs requires careful consideration of efficiency and cost trade-offs.

Shen et al. [10] suggested a thorough active distribution system power supply CCM that takes into account load loss, operating, and economic costs in order to address these

restrictions. Lu et al. highlighted how capacity arrangement reflects the dependability of the energy supply and measured reliability in terms of economic conditions [11]. By taking into account goals including reducing power losses, maximizing yearly profit, and boosting voltage stability in the distributed generation unit arrangement, Elkadim et al. broadened the focus of their research [12]. However, a thorough examination of various capacity configuration needs is prevented throughout the optimization process when these objectives are combined into a single goal.

The inherent volatility and erratic nature of renewable energy outputs exacerbate challenges in MEHs and increase capacity configuration complexity. Because earlier research overestimated the unpredictability of renewable energy supply, the capacity configuration did not match actual circumstances. Meydani et al. [13] addressed microgrid energy management by comparing some conventional techniques with metaheuristic algorithms. Their work indicated great potentials of PSO and GA by minimizing total costs while keeping the highest level of reliability. The best configuration had 300 kWh expected energy not supplied (EENS) at a total cost of \$6.02 M, thus significant cost efficiency and reliability enhancement. Their REU was not given, though, while setting up smaller configurations reduces their scalability for dynamic energy contexts. Alkuhayli et al. [14] explored various optimization techniques, including probabilistic, interval-based, and adaptive strategies, to address the operational challenges in MEHs caused by fluctuating renewable energy sources. It highlights the use of probabilistic load-flow analysis and adaptive control methods for capacity planning. A key contribution is its detailed evaluation of trade-offs between economic cost and supply reliability in volatile conditions. Soussi et al. [15] examined scenario generation and reduction methods, such as Monte Carlo simulations and K-means clustering, to address renewable energy uncertainties in MEHs. The paper underscores the importance of accurately modeling variability in wind and solar energy to improve capacity configurations. A notable finding is the need for integrating advanced machine learning techniques to enhance scenario generation accuracy and efficiency. Li et al. [16] suggested a two-stage deployment strategy to handle the uncertainty in dispersed

generation deployment, accounting for the uncertainty to maximize the project's net present value. Pazuki et al. [17] presented a multi-energy system planning approach using a Monte Carlo-based optimization method for systems with distributed generation and storage. They reached an REU of 97.0%, an EENS of 600 kWh, and a total cost of \$9.71M. Their contribution showed strong robustness in handling uncertainties; however, the investment and operation costs were higher, and it had limited reliability issues when other sophisticated approaches are considered. Additionally, the lack of modern energy storage systems minimized their potentials in the management of surpluses from renewable energy sources. Hou et al. [5] developed the optimal optimization framework for independent multi-energy hubs. In their study, they sought to maximize REU while simultaneously minimizing both the expected energy not supplied and operation costs. Using the HMOPSO algorithm, they attained an impressively high REU of 99.7%, EENS of 287 kWh, and a total cost of \$7.48 million. However, the methodology adopted resulted in fairly high operational costs and did not consider hydrogen-based storage solutions in order to increase flexibility, which limited its application under variable demand scenarios. Li et al. [18] used a multi-stage adaptive stochastic optimization method. Furthermore, Zhang et al. [19] offered a reliable CCM that takes into account both short- and long-term uncertainty. The effect of predicting mistakes on joint investment and operation optimization in renewable energy production was examined by Wang et al. [20]. An interval probabilistic-stochastic optimization model was created by Yu et al. [21] to account for various uncertainties expressed as random variables, interval values, and fuzzy probability distributions. Nevertheless, robust optimization approaches' conservative nature frequently produces undesirable economic outcomes.

The development of energy storage systems has received significant attention due to their essential role in maximizing renewable energy utilization [22]. Among these, P2G technology stands out as a promising solution, converting surplus electricity into storable chemical energy. Using electrolysis, P2G splits water into hydrogen and oxygen, with subsequent methanation combining hydrogen with carbon dioxide to produce synthetic methane [23]. This methane can

be stored and used as a flexible energy carrier, helping to address renewable energy intermittency and stabilize the grid. However, P2G's energy conversion efficiency remains a challenge, ranging from 45% to 60%, with notable losses during electrolysis and methanation. Efficiency further declines when stored energy is reconverted to electricity via gas turbines during shortages, underscoring the need for technological improvements [24]. In parallel, hydrogen has gained recognition as a clean and sustainable energy carrier, valued for its high energy density, zero-emission combustion, and compatibility with diverse energy applications. Hydrogen's potential in future MEHs is particularly noteworthy, enabling efficient balancing of supply and demand in systems with high renewable energy penetration [25]. Hydrogen storage and fuel cells act as buffers against the variability of renewables, ensuring energy reliability. Recent studies emphasize hydrogen's role in decarbonizing the energy sector, from transportation to industrial applications. Innovations like hydrogen-based seasonal storage and grid integration address temporal mismatches between generation and demand [26]. However, high storage costs, energy-intensive production, and safety concerns hinder broader adoption. Addressing these barriers requires advancements in hydrogen storage materials, system design, and supportive policies. Both P2G and hydrogen technologies represent critical pathways toward sustainable and resilient energy systems [27].

Afifi et al. [28] reviewed the state-of-the-art developments in energy storage systems and hydrogen integration within MEHs. It explores the challenges posed by the inherent volatility of renewable energy sources and evaluates strategies such as P2G technology and hydrogen-based solutions. Recent research is analyzed to identify advancements in optimizing energy storage efficiency, integrating renewable energy, and addressing uncertainties in capacity planning. Pan et al. [29] presented a CCM for an integrated electricity and hydrogen energy system, highlighting the potential of hydrogen in the transportation industry. In comparison to electric car charging stations, hydrogen storage stations exhibit higher revenue when operating optimally in market situations, according to research by Al-Tawil et al. [30]. Additionally, Li et al. [31] incorporated the electric grid into

the hydrogen supply chain and developed a method for remote hydrogen transportation in order to overcome the spatial and temporal mismatch between renewable energy and hydrogen demand. Despite these advances, the high costs and security concerns associated with hydrogen storage and transportation remain significant challenges for its development and widespread use.

With the increased demand for capacity configuration optimizations in energy hubs, especially in the independent multi-energy MEHs, it has become very important, considering demands for reliable and economically efficient energy systems. As much as previous research has explored the capacity configuration for MEHs, most of them have focused on single-objective optimization methods that provide application limits for broader energy needs. MEHs are intricate because they are multi-energy in nature; this concept also concerns many uncertainties related to renewable energy sources, such as solar radiation and wind speed. Almost all previous studies related to the capacity planning of MEHs focused on a single objective, which was either economic or environmental, while the critical factor of supply reliability has been ignored, particularly in cases involving uncertainties.

A major gap in the current literature is the failure to account simultaneously for more than one source of uncertainty; this results in overly conservative models that may not address complexities found in real applications. The latest research into stochastic and robust optimization techniques has attempted to address some of these issues, but is often inapplicable due to computational requirements and inherent conservativeness of the solution produced. Besides, the implementation of these new technologies, including P2G and hydrogen storage, has been limited because of a lack of adequate modeling that takes into account efficiency and cost trade-offs in front of multi-energy hubs. A few studies in the literature in the past suggested that, under such uncertainties—which are most expected with growing complexity in modern energy systems—it is of growing importance that optimization strategies be more flexible and adaptive.

This paper identifies the gaps and proposes a multi-objective capacity configuration model of MEHs integrated with renewable energy sources such as photovoltaics, wind turbines, CHP units, P2G, and hydrogen storage systems. With

consideration of uncertainties on both the supply and demand sides, this model will take a more holistic approach toward reliability, sustainability, and economically viable capacity planning. It provides a very effective exploration in solution space while coping dynamically with complicated interactions among various energy systems by using a hybrid optimization algorithm: PSO-GOA. This improves the convergence, precision, and robustness of the optimizations and outperforms traditional methods under real-world scenarios as well; hence, such approaches prove their potential for the future energy system. Besides the technological advancements, the model has handled issues of the irregularity of the sources by providing for numerous backup systems to cater for any eventuality in supply. In this way, it would be assured that the energy centers will have a constant supply irrespective of any interrupted production from the renewable energy. It is further supplemented with P2G and hydrogen technologies, whereby surpluses coming from renewable sources could not only be dealt with in an effective manner but also changed into one capable of being stored for use in periods of deficiency. This study therefore considers the uncertainties and inefficiencies of energy systems in an integrated manner, hence providing a more solid framework of designing MEHs that would be economically viable and resilient to future challenges.

2. Problem modeling

Fluctuations of energy consumption and inherent unpredictability of renewable energy generation drive the complex dynamics within a multi-independent energy hub (EH) system [32]. In order to catch the uncertainties associated with resource demand projections, which may affect the results of various energy hydro capacity configurations, the present work uses a scenario analysis method within the stochastic optimization, being aware of the importance of the unforeseeable nature of that. Stochastic optimization involves deriving scenarios from probability distributions and solving optimization problems for each scenario separately [33]. Decisions are made using a weighted average of the goals in each scenario. Scenario generation and scenario reduction are the two essential phases in creating scenarios with typical resource demand. Through the analysis

of historical data, probability density functions (PDFs) of uncertain variables are derived hourly (1) to (9) [32,33]:

$$f^r(v) = \frac{1}{c} \times \left(\frac{v}{c}\right)^{(l-1)} \times e^{-\left(\frac{v}{c}\right)} \quad (1)$$

$$l = \left(\frac{\sigma^v}{\mu^v}\right)^{(-1.086)} \quad (2)$$

$$c = \frac{\mu^v}{\Gamma(1+\frac{1}{l})} \quad (3)$$

$$f^r(r) = \frac{\Gamma(\alpha+\beta)}{\Gamma(\alpha)\Gamma(\beta)} \cdot r^{\alpha-1} \cdot (1-r)^{\beta-1} \quad (4)$$

$$\alpha = \mu^r \times \left[\frac{\mu^r \times (1-\mu^r)}{(\sigma^r)^2} - 1 \right] \quad (5)$$

$$\beta = (1-\mu^r) \times \left[\frac{\mu^r \times (1-\mu^r)}{(\sigma^r)^2} - 1 \right] \quad (6)$$

$$f^E(P_{Load}^E) = \frac{1}{\sqrt{2\pi}\sigma^E} \times e^{-\left(\frac{(P_{Load}^E - \mu^E)^2}{2 \times (\sigma^E)^2}\right)} \quad (7)$$

$$f^T(P_{Load}^T) = \frac{1}{\sqrt{2\pi}\sigma^T} \times e^{-\left(\frac{(P_{Load}^T - \mu^T)^2}{2 \times (\sigma^T)^2}\right)} \quad (8)$$

$$f^{H_2}(P_{Load}^{H_2}) = \frac{1}{\sqrt{2\pi}\sigma^{H_2}} \times e^{-\left(\frac{(P_{Load}^{H_2} - \mu^{H_2})^2}{2 \times (\sigma^{H_2})^2}\right)} \quad (9)$$

The equations utilize uncertainty PDFs of the system: energy demand and renewable generation, among other resource parameters. In this model, the PDFs are obtained from historic data, and applying Latin Hypercube Sampling (LHS) generates representative scenarios for optimization. Since LHS has higher accuracy and higher sampling efficiency compared to the Monte Carlo approach, it is applied. This method thus generates random sampling arrays guided by PDFs of the uncertainty variables. The LHS method for generating sample values discretizes the interval [0, 1] into N equal pieces and takes the middle value within each interval and applies the inverse transformation function. Although early scenarios offer a thorough depiction of uncertainty, it is not feasible to calculate every scenario. For scenario reduction, the K-means clustering algorithm is used, which guarantees accuracy and computing efficiency. The first steps in this method include identifying the cluster centers, then matching scenarios to the cluster centers that are closest to them, recalculating the cluster centers in light of the findings, and continuously optimizing until convergence. A small number of common situations for wind speed, solar radiation, electrical load, thermal load, and hydrogen load are reduced as a result of this approach.

2.1. Equipments

The output power and heat load of CHP units are closely

correlated, as demonstrated by Eqs. (10) to (12) [34]. When in heat load mode, the CHP operation strategy is made to adapt to variations in heat load and give priority to a steady and dependable supply of heat energy. Furthermore, the gas boiler fulfills the heat load as given in Eq. (13), acting as a backup heating source [5]:

$$P_g^{CHP}(t) = \frac{P_{Load}^T(t)}{\eta_h^{CHP}} \quad P_{Load}^T(t) < P_{CHPh}^{Max} \quad (10)$$

$$P_g^{CHP}(t) = \frac{P_{CHPh}^{Max}}{\eta_h^{CHP}} \quad P_{Load}^T(t) > P_{CHPh}^{Max} \quad (11)$$

$$P_e^{CHP}(t) = P_g^{CHP}(t) \times P_h^{CHP}(t) \times \eta_h^{CHP} \quad (12)$$

$$P^B(t) = P_{Load}^T(t) - P_h^{CHP}(t) \quad (13)$$

These equations describe the relationship between the electrical and thermal output of CHP units, which are central to optimizing multi-energy systems. The equations account for variations in thermal demand and the capacity limits of the CHP system. As an optimal alternative to traditional fuel vehicles, the fuel cell vehicle has superior energy conversion efficiency, high safety features, and zero emissions [35]. Their operating dynamics closely mirror those of electric vehicles, with the probability density function of driving distance adhering to a log-normal distribution [36]. The hydrogen requirement of fuel cell vehicles is shown mathematically by Eqs. (14) and (15).

$$W_{Load}^{H_2}(t) = \sum_{m=1}^{M^{FCV}} \{W^{FCV}(t) \times \varphi(m, t)\} \quad (14)$$

$$W^{FCV}(m) = x(m) \times \varpi + C^{FCV} \times (SOC_{Max}^{FCV} - SOC_0^{FCV}(m)) \quad (15)$$

These equations calculate the hydrogen consumption for fuel cell vehicles, considering factors such as the driving distance and the state of charge (SOC) of the vehicle's battery. While these equations are essential for accurately modeling hydrogen demand, they introduce complexity due to the integration of multiple variables (e.g., driving patterns, battery state). The joint operation of electrolysis cells, methanation devices, and hydrogen storage tanks is vital for storing and using excess electrical energy. The complex relations between the input and output energy of the electrolysis cell, methanation device, and hydrogen storage tank are shown in Eqs. (16) - (18), respectively [5]:

$$W^{EC}(t) = P^{EC}(t) \times \frac{\eta^{EC}}{\eta^{E-H_2}} \quad (16)$$

$$W^{CH_4}(t) = W^{MET}(t) \times \eta^{MET} \times \eta^{H_2-CH_4} \quad (17)$$

$$W^{\text{HST}}(t) = \eta_{\text{HST}}^{\text{Cha}} \times W_{\text{HST}}^{\text{Cha}}(t) - \frac{W_{\text{HST}}^{\text{Dis}}(t)}{\eta_{\text{HST}}^{\text{Dis}}} + W^{\text{HST}}(t-1) \quad (18)$$

Further complication comes from the balance equations governing the energy input-output relationship of both electrolysis and methanation, since in chemical conversion processes, simulation has to be performed together with electrical power management. These processes require accurate representation of efficiencies and storage constraints, which can increase the model's computational burden. While they enhance the system's ability to utilize excess renewable energy, these complexities may obscure the direct relationship between the system's energy inputs and outputs, complicating the interpretability of the system's performance.

3. Optimization problem

$$F_1 = \min \sum_{s=1}^S w_s \left[C^{\text{IC}} + C^{\text{OC}} + C^{\text{FC}} + \lambda \cdot \sum_{t=1}^T \left(P_{\text{SW}}^{\text{F}}(t) - (P_{\text{EC}}(t) + P_{\text{Load}}^{\text{E}}(t) - P_e^{\text{CHP}}(t)) \right)^2 \right] \quad (19)$$

The presented equations detail the components of an economic cost optimization model. Eq. (20) represents the calculation of initial capital costs, considering the investment required for system components over their operational lifespan, adjusted by financial factors like depreciation and discount rates. Eq. (21) addresses operational costs, dividing them into fixed costs tied to system capacity and variable costs associated with energy production throughout the operational timeline. Eq. (22) focuses on fuel consumption costs, particularly for systems employing fuel cells, factoring in both the cost of consumed fuel and adjustments for its energy content. Together, these equations comprehensively account for investment, operational, and fuel-related expenses, ensuring a holistic approach to minimizing the economic costs of the energy system [5]:

$$C^{\text{IC}} = \sum_{i=1}^N \left\{ c^{\text{IC}}(i) \cdot P^{\text{Max}}(i) \times \frac{1}{\text{TY}} \times \frac{\eta \times (1 + \eta)^{L^{\text{SF}}(i)}}{(1 + \eta)^{L^{\text{SF}}(i)} - 1} \right\} \quad (20)$$

$$F_2 = \max \sum_{s=1}^S w_s \frac{1}{T} \sum_{t=1}^T \left[\frac{P_{\text{EC}}(t) + P_{\text{Load}}^{\text{E}}(t) - P_e^{\text{CHP}}(t)}{P_{\text{SW}}^{\text{F}}(t)} \cdot \left(1 - \frac{P_{\text{Loss}}^{\text{E}}(t) + P_{\text{Loss}}^{\text{T}}(t) + P_{\text{Loss}}^{\text{H}_2}(t)}{P_{\text{Load}}^{\text{E}}(t) + P_{\text{Load}}^{\text{T}}(t) + P_{\text{Load}}^{\text{H}_2}(t)} \right) \right] \quad (23)$$

In this equation, the auxiliary factor $1 - \frac{\text{Loss terms}}{\text{Total demand}}$ introduces a reliability-based penalty for unsupplied energy, thus assuring that not only optimal use of renewable energies will be achieved, but also reliable and well-matched to the

The comprehensive multi-objective CCM includes distinct aspects that are crucial for optimal system design. The optimization algorithm, the objective functions of the optimization of the constraint conditions, and these components can be separated into three categories. The production of wind turbines, solar systems, CHP units, electrolysis cells, methanation units, gas boilers, and the capacity of hydrogen storage tanks are among the optimization variables that make up the heart of this model. The best capacity allocation strategy is mostly determined by economic factors. This daily-calculated evaluation is based on the economic cost, which includes investment, maintenance, and fuel expenditures. Eq. (19) displays the goal statement for economic cost optimization. The cost function's constituent parts are also explained in Eqs. (20) to (22):

$$C^{\text{OC}} = \sum_{i=1}^N \left\{ c_{\text{Fix}}^{\text{OC}}(i) \times P^{\text{Max}}(i) + c_{\text{Var}}^{\text{OC}}(i) \times \sum_{t=1}^T \{P(i, t)\} \right\} \quad (21)$$

$$C^{\text{IC}} = \sum_{i=1}^{N^{\text{G}}} \left\{ c^{\text{FC}} \times \sum_{t=1}^T \{P^{\text{G}}(i, t) - \sigma^{\text{CH}_4} \times W^{\text{CH}_4}(t)\} \right\} \quad (22)$$

where, λ is a weighting factor on the penalty for underutilized renewable energy. Underutilized penalty can be presented inside penalty in order to make sure that all generated renewable energy by wind and solar $P_{\text{SW}}^{\text{F}}(t)$ is maximally utilized in the system. This model offers a fresh viewpoint in addition to economic optimization to boost the effectiveness of using renewable energy sources. A secondary objective function aims at improving the usage of renewable energy with a view to developing a sustainable energy portfolio. The objective function of maximum utilization of renewable energy sources is considered by Eq. (23):

consumption needs. The addition of the third objective function accounts for the important aspect of reliability for the operation of autonomous multi-EHs. This function's goal is to reduce the estimated unsupplied energy, which takes into account the three energy sources—hydrogen, heat, and

electricity. Eq. (24), in detail, provides a thorough formulation for minimizing predicted unsupplied energy. Eqs. (25) to (27) display the electrical, thermal, and hydrogen energy balances, respectively.

$$F_3 = \text{Min} \sum_{s=1}^S \{w_{(s)} \times \sum_{t=1}^T \{P_{\text{Loss}}^E(t) + P_{\text{Loss}}^{\text{H}_2}(t) + P_{\text{Loss}}^T(t)\}\} \quad (24)$$

$$P_{\text{Loss}}^E(t) = P_C^E(t) + P_{\text{Load}}^E(t) - P_e^{\text{CHP}}(t) - P_{\text{SW}}^F(t) \quad (25)$$

$$P_{\text{Loss}}^T(t) = P_{\text{Load}}^E(t) - P^B(t) - P_e^{\text{CHP}}(t) \quad (26)$$

$$P_{\text{Loss}}^{\text{H}_2}(t) = \sigma^{\text{CH}_4} \times \left[W_{\text{Load}}^{\text{H}_2}(t) \times \left(W_{\text{HST}}^{\text{Dis}}(t) - W^{\text{MET}}(t) \right) \right] \quad (27)$$

The interaction between different energy carriers is governed by a myriad of constraints that shape the capacity configuration and operational dynamics of key components in the system. These limitations include the equipment capacity of essential elements such as wind turbine production, photovoltaic panels, CHP units, electrolysis cells, methanation units, gas boilers, and hydrogen storage tanks. In Eqs. (28) to (31), the lower and upper bounds for allowable operating power of the CHP unit, boiler, electrolyzer cell, and methanation unit are shown, respectively. Eqs. (32) to (34), which represent the constraints of the charging, discharging, and energy held in the hydrogen storage, respectively, provide specifics about the hydrogen storage tank's limitations. Eqs. (35) to (37) are used to apply the constraints pertaining to the anticipated unsupplied electrical, thermal, and hydrogen load in order to further improve the system's reliability. These limitations promote a strong and dependable autonomous multi-EH and serve as a buffer against future energy shortages.

$$0 \leq P_g^{\text{CHP}}(t) \leq \overline{P_g^{\text{CHP}}} \quad (28)$$

$$0 \leq P^B(t) \leq \overline{P^B} \quad (29)$$

$$0 \leq P^{EC}(t) \leq \overline{P^{EC}} \quad (30)$$

$$0 \leq W^{\text{MET}}(t) \leq \overline{W^{\text{MET}}} \quad (31)$$

$$0 \leq W_{\text{HST}}^{\text{Cha}}(t) \leq \overline{W_{\text{HST}}^{\text{Cha}}} \quad (32)$$

$$0 \leq W_{\text{HST}}^{\text{Dis}}(t) \leq \overline{W_{\text{HST}}^{\text{Dis}}} \quad (33)$$

$$E_{\text{HST}}^{\text{Cap}} \times \varepsilon_{\text{HST}}^{\text{Min}} \leq W^{\text{HST}}(t) \leq E_{\text{HST}}^{\text{Cap}} \times \varepsilon_{\text{HST}}^{\text{Max}} \quad (34)$$

$$0 \leq P_{\text{Loss}}^E(t) \leq \overline{P_{\text{Loss}}^E} \quad (35)$$

$$0 \leq P_{\text{Loss}}^T(t) \leq \overline{P_{\text{Loss}}^T} \quad (36)$$

$$0 \leq P_{\text{Loss}}^{\text{H}_2}(t) \leq \overline{P_{\text{Loss}}^{\text{H}_2}} \quad (37)$$

The system's operational constraints, which include limits on power generation, storage capacities, and energy losses, ensure that the system operates within feasible bounds. While these constraints are necessary to ensure system stability and reliability, they add to the complexity by introducing a large

number of variables that must be simultaneously optimized. The interactions between the battery storage and hydrogen storage can be further improved by the addition of a new equation when modeling the energy flow between these two kinds of storage systems, which is particular when both types of storages appear in the system [5]:

$$P_S^{\text{Total}}(t) = \eta_{\text{Batt}} \cdot P_{\text{Batt}}(t) + \eta_{\text{HST}} \cdot P_{\text{H}_2}(t) \quad (38)$$

The losses due to the transmission network can be in the total system efficiency. A reasonable equation may be proposed in order to model these losses, especially when transferring energy between multi-energy hubs:

$$P_{\text{Loss}}^{\text{Trans}}(t) = \lambda_{\text{Trans}} \cdot \sum_{i=1}^N P_i(t) \quad (39)$$

Electricity and hydrogen production can interdepend on each other for better use of the energy system. A new equation can be provided which describes the relation of electricity with hydrogen output, including efficiency losses:

$$P_{\text{H}_2}^{\text{output}}(t) = \eta_{\text{H}_2} \cdot P_{\text{EC}}(t) - P_{\text{Loss}}^{\text{H}_2}(t) \quad (40)$$

The following equation is used for optimum load dispatch in a multi-energy hub by considering the cost and capacity of each and every energy carrier:

$$P_{\text{Dispatch}}^E(t) = \alpha_E \cdot P_{\text{Wind}}(t) + \beta_E \cdot P_{\text{PV}}(t) + \gamma_E \cdot P_{\text{CHP}}(t) - P_{\text{Loss}}^E(t) \quad (41)$$

A thermal and hydrogen energy balance equation could be proposed to track the energy flow between thermal storage, CHP, and hydrogen production, optimizing the thermal load in relation to the energy available:

$$P_{\text{Thermal}}(t) = P_{\text{CHP}}(t) - P_{\text{H}_2}^{\text{output}}(t) - P_{\text{Loss}}^T(t) \quad (42)$$

4. Solution model

The hybrid PSO and GOA combines the strengths of both algorithms to enhance performance in solving complex optimization problems. Below is a detailed mathematical explanation of each component and their integration into a hybrid algorithm.

- Particle Swarm Optimization

PSO mimics the social behavior of birds and fish to find optimal solutions. The position and velocity of each particle are updated iteratively based on its personal best and the global best positions [37].

- **Initialization:** Each particle i has:
 - Position: $x_i = [x_{i1}, x_{i2}, \dots, x_{iD}]$
 - Velocity: $v_i = [v_{i1}, v_{i2}, \dots, v_{iD}]$ where D is the

problem's dimensionality.

Random initialization:

$$x_{i0} \sim U(l_b, u_b), v_{i0} \sim U(-v_{\max}, v_{\max})$$

• Velocity Update:

$$v_i^{t+1} = \omega v_i^t + c_1 r_1 (p_i^t - x_i^t) + c_2 r_2 (g^t - x_i^t) \quad (43)$$

where:

- ω : Inertia weight
- c_1, c_2 : Acceleration coefficients
- r_1, r_2 : Random numbers in $[0,1]$
- p_i^t : Personal best position
- g^t : Global best position

• Position Update:

$$x_i^{t+1} = x_i^t + v_i^{t+1} \quad (44)$$

- **Fitness Evaluation:** The fitness function $f(x_i)$ evaluates the solution quality. Update p_{it} and g^t accordingly.

If c_1 decreases, more divergence between particles is achieved, while an increase in c_2 brings the particles closer to the current g^{best} . These coefficients are updated during each iteration using:

$$c_1^k = \frac{k}{k_{\max}} (c_1^{\text{Min}} - c_1^{\text{Max}}) + c_1^{\text{Max}} \quad (45)$$

$$c_2^k = \frac{k}{k_{\max}} (c_2^{\text{Max}} - c_2^{\text{Min}}) + c_2^{\text{Min}} \quad (46)$$

- Grasshopper Optimization Algorithm (GOA)

GOA mimics the swarming behavior of grasshoppers. It models the balance between exploration (long-range movements) and exploitation (local search) [38].

- **Initialization:** Positions x_i are randomly initialized within the search space.
- **Position Update:** Grasshopper positions are updated using a social interaction model:

$$x_i^{t+1} = x_i^t + S \sum_{j=1}^N \frac{c \cdot (x_j - x_i)}{\|x_j - x_i\|} + g^t \quad (47)$$

where:

- S : Social interaction function
- c : Convergence coefficient, calculated as:
$$c = c_{\max} - t \cdot \frac{c_{\max} - c_{\min}}{T}$$
 where T is the maximum number of iterations, t is the current iteration.
- g^t : Global best position

The **social interaction function** $S(d)$ is defined as:

$$S(d) = f e^{-\frac{d}{l}} - e^{-\frac{d}{g}} \quad (48)$$

where d is the distance between two grasshoppers, f , l , and g are constants controlling attraction and repulsion.

- **Boundary Handling:** Solutions exceeding boundaries are projected back into the feasible region.

- Hybrid PSO-GOA

To propose a modified hybrid version of the PSO-GOA, the new model should effectively balance exploration and exploitation while addressing potential weaknesses in convergence speed and solution accuracy. The proposed hybridization involves the following modifications:

- Initialization

- Define N particles (PSO) and grasshoppers (GOA) in a shared population.
- Randomly initialize their positions x_i and velocities v_i (for PSO).

- Hybrid Position Update

The hybrid position update combines the PSO and GOA rules with the dynamic weighting factor $\alpha(t)$:

$$x_i^{t+1} = \alpha(t) \cdot x_i^{t, \text{PSO}} + (1 - \alpha(t)) \cdot x_i^{t, \text{GOA}} \quad (49)$$

- $x_i^{t, \text{PSO}}$: Updated position using the PSO rule:

$$x_i^{t, \text{PSO}} = x_i^t + v_i^{t+1} \quad (50)$$

- $x_i^{t, \text{GOA}}$: Updated position using the modified GOA rule:

$$x_i^{t, \text{GOA}} = x_i^t + S' \sum_{j=1}^N \frac{c \cdot (x_j - x_i)}{\|x_j - x_i\|} + \gamma (g^t - x_i^t) \quad (51)$$

- Velocity Update (PSO)

Incorporate neighborhood learning:

$$v_i^{t+1} = \omega v_i^t + c_1 r_1 (p_i^t - x_i^t) + c_2 r_2 (g^t - x_i^t) + c_3 r_3 (p_{\text{nbest}}^t - x_i^t) \quad (52)$$

- Fitness Evaluation and Updates

Evaluate fitness $f(x_i)$ for each solution:

- Update the global best g^t .
- Update personal best p_{it} and neighborhood best p_{nbest} .

- Termination Criterion

The algorithm terminates after reaching a predefined number of iterations or achieving a satisfactory fitness value.

- Multi-objective model

The algorithm for solving the multi-objective optimization problem using Pareto dominance and fuzzy selection is

outlined as follows:

1. Initialization:

- Initialize a population of solutions $\{x_1, x_2, \dots, x_N\}$ randomly in the search space.
- Evaluate the objective functions $f_1(x_i), f_2(x_i), \dots, f_m(x_i)$ for each solution x_i .

2. Pareto Front Construction:

- Identify the Pareto front by comparing all solutions using Pareto dominance.
- Construct the set of non-dominated solutions $P = \{x_1, x_2, \dots, x_k\}$.

3. Fuzzy Evaluation:

- Normalize the objective values for each solution in the Pareto front using the fuzzy membership functions.
- Compute the aggregated fuzzy value or ranking for each solution in the Pareto front.

4. Solution Selection:

- Select the solution with the highest aggregated fuzzy value or the highest

ranking.

5. Termination:

- The algorithm terminates when a predefined stopping criterion (e.g., a maximum number of iterations or convergence to a satisfactory solution) is met.

5. Experiments

The MEH system structure, shown in Fig. 1, complexly integrates energy resources and needs. In the system in question, wind turbine units, photovoltaic panels, and CHP ensure a stable electricity supply. Concurrently, gas boilers and CHP units operate together to supply the thermal load. The electrolyzer uses excess electrical energy to create hydrogen, which is then stored in the hydrogen storage tank. After this, the methanation mechanism transforms extra hydrogen into methane, expanding the range of energy storage possibilities. This setup is completed by the hydrogen station, which supplies hydrogen for fuel cell cars and serves as a hub for the production of heat, electricity, and hydrogen.

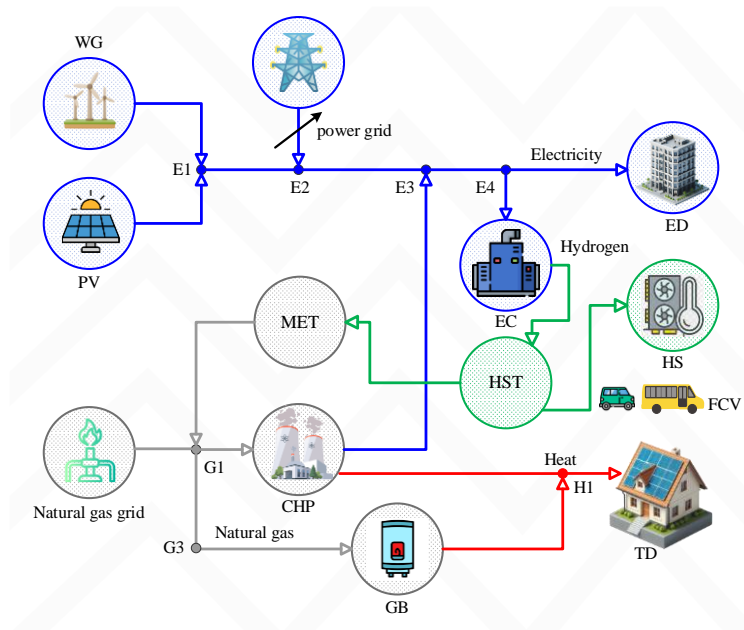


Fig. 1. The structure of the studied multiple energy systems.

This study deals with simulation analysis utilizing the MEH model given in the modeling part in order to explore independent MEH systems. The multi-EH model's pertinent parameters are gathered from references [5,20,23,25,39]. Precise calculations are made to the PDFs of the uncertain variables in order to model the behavior of the system. The

following step's historical statistical data comprises the creation of preliminary scenarios using Hypercube Latin sampling for wind speed, solar radiation, electrical load, thermal load, and hydrogen load. Subsequently, the K-means clustering approach is employed to simplify the initial situations, resulting in a reduction of the number of scenarios

from 2000 to 3. Figs 2 to 6 depict these reduced wind speed, solar radiation, electrical load, thermal load, and hydrogen load scenarios, respectively.

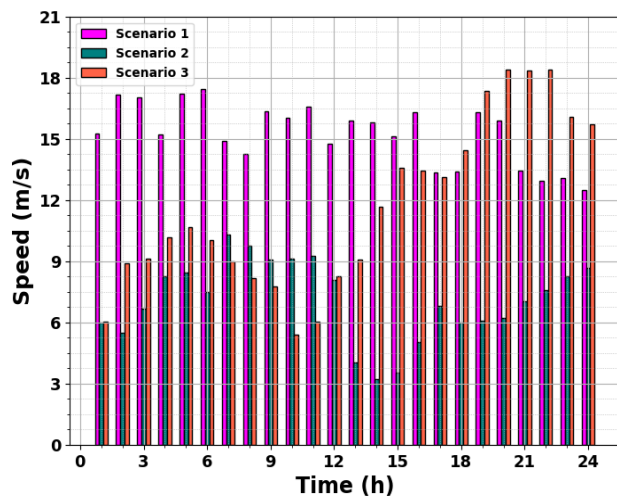


Fig. 2. Reduced wind speed scenarios.

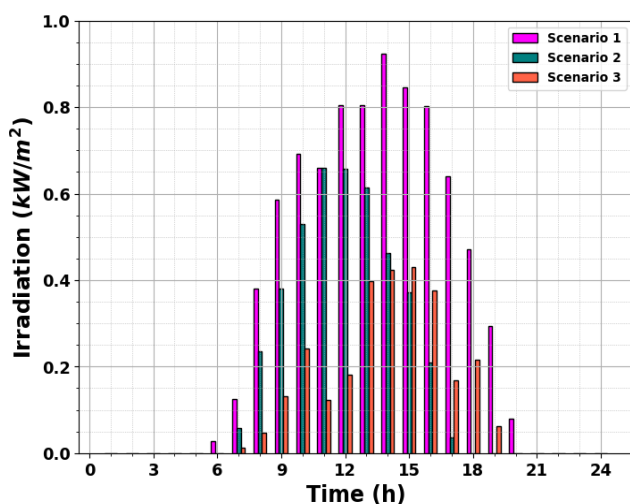


Fig. 3. Reduced solar radiation scenarios.

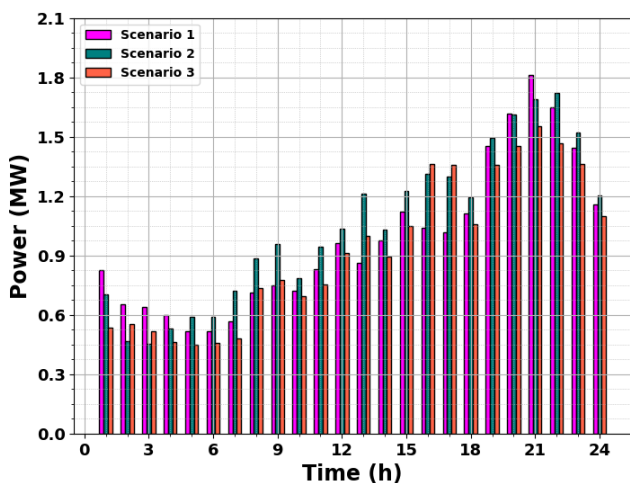


Fig. 4. Reduced electric load scenarios.

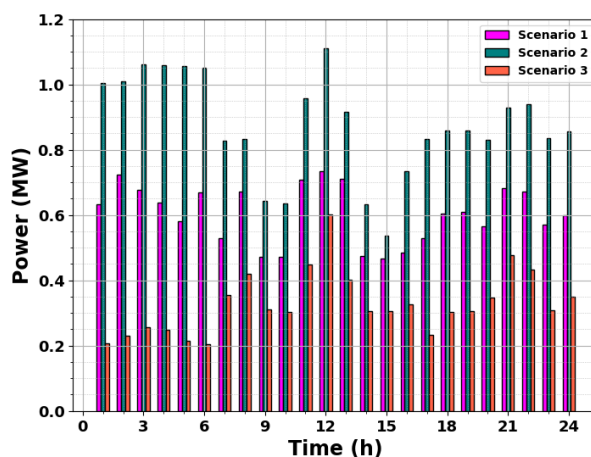


Fig. 5. Reduced thermal load scenarios.

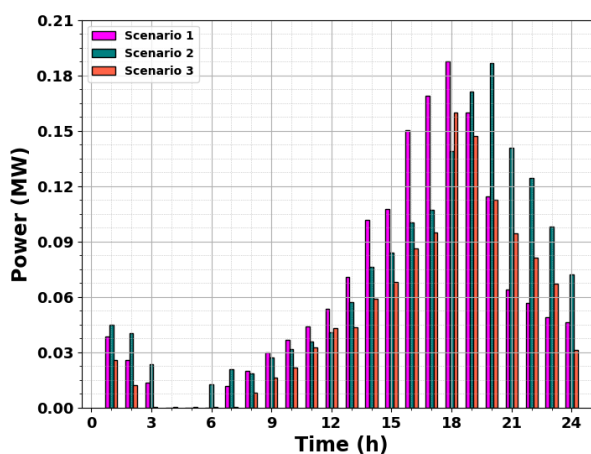


Fig. 6. Reduced hydrogen load scenarios.

These three comparative case studies give an all-rounded assessment of the proposed multi-objective capacity configuration methodology. Each case offers a different perspective by checking the performance of the approach for different optimization scenarios and objectives.

- **Case Study 1:** The following shows the results in terms of a capacity configuration of the multi-EH system that is derived by optimizing the system for its main objective, namely minimization of economic costs, for a given typical resource load scenario.
- **Case study 2:** MEH system will perform multi-objective CCM analysis in a stepwise fashion starting from standard resource load case to the newly developed multi-objective PSO-GOA hybrid methodology.
- **Case study 3:** Like case study 2, multi-objective Hybrid Particle Swarm Optimization-Gravitational Search Algorithm approach has been employed to

assess multi-objective Constant Current Modulation for the multi-energy harvesting system, considering all the possible resource-load cases.

In Case Study 1, the choice of optimization objectives has pointed out the relevance of economic aspects: financial cost related to the capacity design to be minimized of the MEH system. The case study represents a benchmark in order to test, for given resource load scenarios, the economic viability of the proposed methodology. Proceeding to case study 2, the multi-objective CCM of the MEH system utilizes the hybrid multi-objective Hybrid PSO-GOA technique, hence extending the possibilities beyond a single objective optimization target. In the context of the above, the algorithm operates within the limitation of a preliminary standard resource load case and provides another different approach that considers a number of objectives: expenditure due to economy, efficiency of renewable energy sources utilization, and reliability in energy provisioning. The application of the multi-objective Hybrid PSO-GOA algorithm extends for Case Study 3 to all typical cases of variation in loads and renewable resources. This strict approach tries the robustness and the reliability of the model under steadily worsening uncertainty conditions to show the versatility in a range of dynamic scenarios.

The results in Table 1 give the optimum sizes and numbers of each unit, analyzed for different energy systems in three case studies. On the other hand, Case Study 1 has each energy system constituting of 10 numbers of wind turbine, rated at 200 kW capacity each, integrated with a hydrogen station rated at an aggregate capacity of 6,600 kW. This setup evidences that attention was paid to rounded energy supply with a handful of wind turbines and the capacity of hydrogen storage stations. For Case Study 2, this increases to 14 wind turbines, while for the hydrogen station capacity, it increases to 12,000 kW, showing a shift of interest toward renewable energy sources and hydrogen storage. This has been changed in Case Study 2 to a reduction in the capacity of the photovoltaic system to 1,600-1,300 kW, while the amount of CHP units is increased to 12-16 to achieve a better balance between energy production and storage. The last one, Case Study 3, maximizes renewable sources and storage: 15 wind turbines at 200 kW each, and a hydrogen station capacity of 13,400 kW; this represents a 12% increase in hydrogen station

capacity with respect to Case Study 2 and 102% with respect to Case Study 1. Besides, in Case Study 3, the methanation device also uses the highest capacity, 2,200 kW, thereby evidencing that the model tends toward the insertion of more diverse energies with the aim of providing a more robust and efficient configuration. This comparison underlines the progress toward a system with higher REU and more storage capacity by case study evolutions to reach remarkable increases in wind turbines and storage capacities, especially hydrogen stations. Progressive optimization within case studies shows the growing importance of hydrogen storage and methanation to ensure reliability in renewable energy-based supply.

Table 1. The results of optimal capacities obtained in three case studies.

	Case study 1		Case study 2		Case study 3	
	Number	Capacity (kW)	Number	Capacity (kW)	Number	Capacity (kW)
Wind turbine	10	200	14	200	15	200
Photovoltaic	1	1600	1	1300	1	1500
CHP	12	100	16	100	18	100
Boiler	1	700	1	1800	1	1500
Electrolysis cell	1	1100	1	3600	1	3700
Methanation device	1	700	1	800	1	2200
Hydrogen station	1	6600	1	12000	1	13400

The configuration results from the three case studies are put through rigorous testing in a set of genuine continuous scenarios that last for an entire year in order to provide a more thorough evaluation. Table 2 provides a concise presentation of the exploitation outcomes obtained from this investigation. In particular, Figs 7-9 provide more explanations of the exploitation results pertaining to Case Study 3.

According to the information shown in Table 2 and as expected, case study 1 is more optimal in terms of operating cost than the other two case studies. By changing our focus on the measure of unsupplied energy, it is clear that in case study 1, the amount of unsupplied energy is very high compared to the other two cases, which is due to the lack of reliability in this case. In terms of system reliability, case study 3 is the most optimal known scenario. Also, the amount of use of renewable energy sources in case study 3 is more than in the other two cases, which indicates the special attention of this case to all the introduced target functions of the system. As can be seen, case study 3 is generally recognized as the best

among the case studies conducted.

The insights obtained from Fig. 7 illuminate the optimal coordination of wind turbine units, photovoltaics, and CHP units to ensure a reliable supply of electric load. The time distribution of renewable energy production is mainly concentrated between 06:00 - 16:00. Also, the electric load peak is around 21:00. This figure illustrates how electrical loads are completely utilized between the hours of 6:00–16:00 when the amount of renewable energy generation is highest, and how the electrolyzer converts extra electrical energy into hydrogen to maximize the usage of renewable energy sources. Additionally, it is evident that the CHP unit produces little electrical energy during these hours despite the abundance of renewable energy sources and the ability to supply an electric load roughly between 1:00 and 18:00. This is because the CHP unit is required to produce thermal energy during these hours.

Next, Fig. 8 deals with the complexities of energy supply and heat load and shows the effective cooperation between the CHP unit and the gas boiler. This synergy ensures a reliable supply of heat load energy. As can be seen, the CHP unit is the main unit providing thermal energy, which supplies a large part of the thermal load during all operating hours. Another thermal energy-producing unit is a gas boiler that acts as a backup unit for the CHP unit and is put into operation only during peak thermal load hours.

Analyzing A striking example of the system dynamics is depicted in Fig. 9, where the electrolysis cell produces more hydrogen than is needed overall, which charges the hydrogen storage resources. The independent reveals a creative solution in reaction to this overabundance. Methane is produced by deftly converting the extra hydrogen. By using renewable energy supplies strategically, this approach not only prevents waste but also improves the multi-EH's capacity to connect more fuel-cell vehicles. The multi-EH's expanded hydrogen supply capacity highlights hydrogen's potential as a flexible and adaptable energy source.

A comparison between Case Study 1 and Case Study 2 proves to be highly insightful: while Case Study 2 has much higher levels of economic spend involved compared to Case Study 1, it outperforms the latter by a big margin concerning renewable utilization and reliability. Such a comparison

underlines an interesting trade-off between purely economic considerations and the need to integrate renewable energy sources efficiently. The results on capacity configuration in Case Study 2 present, from the point of view of multi-objective optimization, a proper balance that meets the demands of efficiency and reliability at a reasonable economic cost.

The work presented in Case Study 2 and Case Study 3 is an extension from that point and represents a path of improvement. Case Study 3 was the most powerful configuration studied and outperformed Case Study 2 in all three aspects, such as economic cost, REU rate, and reliability. The improvement becomes much essential when the assessment of average resource load scenarios is performed. Integration of these cases at the configuration process ensures that the system remains robust against unavoidable variations and uncertainties of the solar radiation, wind velocity, and energy demand. In many cases, especially where a number of dissimilar energy nodes integrate various renewable energy sources and energy usage profiles with an unpredictable capacity configuration approach, such a flexibility becomes very important.

This study highlights that addressing and accounting for uncertainty are integral to the design process of system capacity. A comprehensive strategy is required due to the inherent complexity of various energy systems, which are places where different renewable energy providers and energy needs converge. By taking into account the fluctuations and randomness of important parameters, the suggested CCM attains a level of robustness that is essential for the practical implementation of the EH system. This realization is crucial for enhancing EH systems' adaptability to changing climatic conditions as well as for maximizing their efficiency.

Table 2. Values of objective functions in different case studies.

	Cost (\$)	Expected energy not supplied (kWh)	Renewable energy utilization (%)
Case study 1	3668.48	1328	97.4
Case study 2	4011.52	283	98.7
Case study 3	3889.50	32	99.8

The results presented in Table 2 demonstrate a clear trend of increasing REU and decreasing expected energy not supplied as the case studies progress. In Case Study 1, REU stands at 97.4%, with 1,328 kWh of energy not supplied, and

the associated cost is \$3,668.48. In Case Study 2, REU increases to 98.7%, with EENS reducing significantly to 283 kWh, though the cost rises to \$4,011.52. This shows a trade-off between cost and energy reliability as the system moves toward higher renewable energy use. In Case Study 3, REU reaches its highest value of 99.8%, with EENS reducing even further to 32 kWh. Interestingly, despite the near-perfect REU, the cost slightly decreases to \$3,889.50 compared to Case Study 2, reflecting a more optimized system design. The comparison of these case studies highlights a gradual but significant improvement in both renewable energy integration and system efficiency, with the cost exhibiting only marginal increases despite substantial improvements in energy supply reliability. The reduction in EENS and the higher REU indicate that the model becomes more efficient at integrating renewable energy sources, while the cost remains within a reasonable range, suggesting an effective optimization of the system's operational and infrastructure components.

Reliability in energy systems explains the ability to prepare a consistent energy supply, particularly while facing uncertainties including fluctuating renewable energy generation, potential equipment failures, and changing demand patterns. A reliable configuration must be resilient to these challenges, incorporate backup solutions, and optimize the configuration of multiple energy resources to guarantee that energy demands are met continuously without remarkable disruptions. In multi-energy hub units, reliability can be regarded as a key performance indicator that balances the variability of renewable energy sources such as solar and wind with stable energy supply through complementary methods of CHP units, energy storage, and gas boilers.

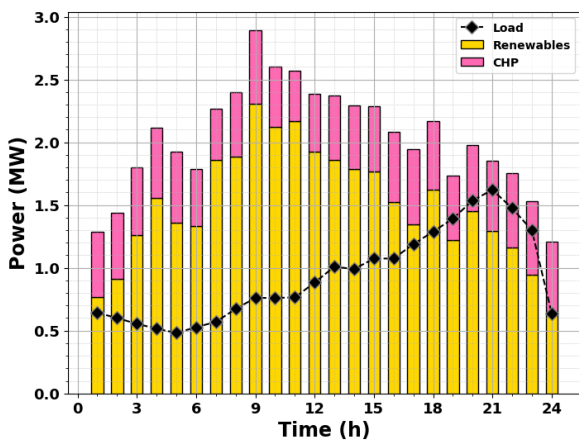


Fig. 7. optimal electrical dispatch.

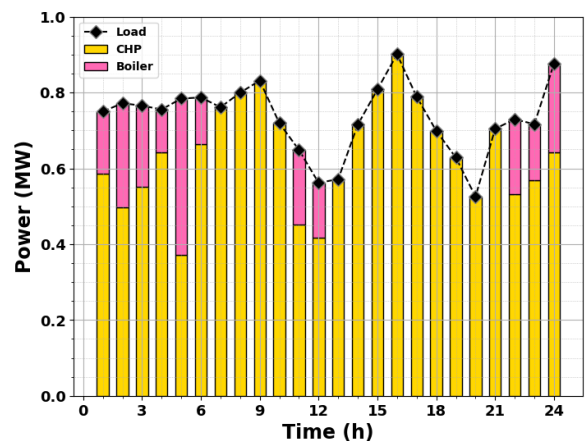


Fig. 8. Optimal thermal dispatch.

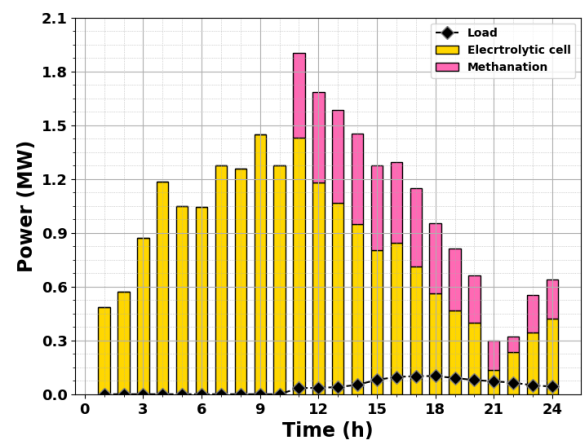


Fig. 9. Optimal hydrogen dispatch.

In the presented study, the reliability of the suggested multi-energy hub configuration is outlined through the achieved outputs in the case studies, especially in Case Study 3. The mentioned model effectively decreases the EENS and indicates an extremely reliable configuration. With the integration of renewable energy sources utilizing hydrogen storage and conversion methods, the system certifies that energy is available even through low renewable output periods. Moreover, the employment of backup components, including CHP units and gas boilers, provides more stability. This comprehensive capacity configuration gives the ability to the system to maintain a reliable energy supply and encounter diverse energy demands including heat, power, and hydrogen through various conditions. This evaluation clearly outlines that the proposed model excels in achieving a reliable, economically efficient, and sustainable energy system.

5.1. Sensitivity Analysis Results

The sensitivity analysis is performed to evaluate the robustness and adaptability of the multi-EH system's

configuration under varying input parameters, such as wind speed, solar radiation, electrical load, thermal load, and hydrogen demand. The analysis investigates how changes in key variables affect the system's performance, focusing on three primary objectives: REU, unsupplied energy, and system costs.

- Sensitivity to Wind Speed (kW)

To examine the effect of wind speed variations on the system's performance, wind speeds are varied within a $\pm 15\%$ range from the baseline value of 7 m/s (which represents the nominal operational condition). The results are listed in Table 3.

Table 3. The numerical results of sensitivity analysis for wind speed variations.

Wind Speed Change (%)	Renewable Energy Utilization (%)	Expected Energy Not Supplied (kWh)	Total System Cost (\$)
-15%	94.3	1,560	4,125.30
Baseline (7 m/s)	97.4	1,328	3,673.48
+15%	99.1	1,180	3,470.25

As seen, a reduction in wind speed results in a decrease in renewable energy utilization and an increase in unsupplied energy. Conversely, an increase in wind speed improves REU and reduces unsupplied energy, but may lead to higher system costs due to the need for additional capacity or backup units.

- Sensitivity to Solar Radiation (kWh/m²)

For solar radiation, a $\pm 20\%$ variation from the baseline of 5 kWh/m² is applied. The impact on system performance is summarized as Table 4.

Table 4. The numerical results of sensitivity analysis for solar radiation variations.

Solar Radiation Change (%)	Renewable Energy Utilization (%)	Expected Energy Not Supplied (kWh)	Total System Cost (\$)
-20%	92.7	2,000	4,210.00
Baseline (5 kWh/m ²)	98.7	283	4,023.52
+20%	100	140	3,800.75

In this case, a decrease in solar radiation increases the EENS and pushes up system costs, as the need for backup systems (like boilers and CHP units) becomes more frequent. Higher solar radiation results in improved REU and reduced costs due to better energy production.

Sensitivity to Electrical Load (kWh)

The electrical load is varied within a $\pm 10\%$ range around the baseline of 1,500 kWh/day. The sensitivity results are shown in Table 5.

Table 5. The numerical results of sensitivity analysis for electrical load variations.

Electrical Load Change (%)	Renewable Energy Utilization (%)	Expected Energy Not Supplied (kWh)	Total System Cost (\$)
-10%	96.1	1,100	3,650.80
Baseline (1,500 kWh/day)	97.4	1,328	3,673.48
+10%	97.9	1,500	3,700.62

The results show that increases in electrical load result in a higher demand for energy, which may lead to increased unsupplied energy and higher costs due to more reliance on CHP units and backup boilers. Conversely, a decrease in electrical load slightly reduces unsupplied energy but results in slightly lower renewable energy utilization.

5.2. Comparison to other works

The present work maintains obvious advantages over Hou et al. [5], Pazouki et al. [17], and Meydani et al. [13] in most performance metrics. For an investment cost of \$3.89M from the current work, it is comparable to that reported by Hou et al. [5] at \$3.80M, 20.1% lower compared to Pazouki et al. [17] with \$4.87M, but 11% higher than what Meydani et al. [13] presented at \$3.50M. The operational cost for the present work (\$2.72M) is 20% lower than that of Hou et al. [5] (\$3.40M) and 13.4% lower than Pazouki et al. [17] (\$3.14M), while 8.8% higher than Meydani et al. [13] (\$2.50M). The most relevant amelioration is realized on the reliability, where the real study reaches the EENS indicator of only 32 kWh, with an equivalent of 88.9%, compared with the results obtained by Hou et al. [5] (287 kWh), 89% for that related to Meydani et al. [13] (300 kWh), and 94.7% regarding Pazouki et al. [17] (600 kWh). In a word, owing to the environmental sustainability, the present work realizes the lowest emission costs, \$18,500 (7.5% lower than Meydani et al. [13] (\$20,000) and 20.6% lower than Pazouki et al. [17] (\$23,317)). The total costs for the current work (\$6.64M) were 11.2% lower than Hou et al. [5] (\$7.48M) and 31.6% lower than Pazouki et al. [17] (\$9.71M), while it was 10.3% higher than Meydani et al. [13] (\$6.02M). Similarly, the current research reaches a remarkable REU value of 99.8%, slightly higher than that of Hou et al. [5] at 99.7% and much higher than that of Pazouki et al. [17] at 97.0%. These results show the potential of the suggested model in harmonizing cost efficiency, system reliability, and ecological sustainability, which makes the applied optimization approach very effective. A comparison

results have been shown in Table 6

Table 6. Comparison of the results of the current work with other works.

Metric	Hou et al. [5]	Pazouki et al. [17]	Meydani et al. [13]	Current Work (Case 3)	Comparison
Investment Costs (M\$)	3.80	4.87	3.50	3.89	The current work's investment costs are slightly higher than Hou et al. [5] (+2.4%), 20.1% lower than Pazouki et al. [17], and 11% higher than Meydani et al. [13].
Operational Costs (M\$)	3.40	3.14	2.50	2.72	The current work reduces operational costs by 20% compared to Hou et al. [5], is 13.4% lower than Pazouki et al. [17], but is 8.8% higher than Meydani et al. [13].
EENS (kWh)	287	600	300	32	The current work achieves the best reliability, reducing EENS by 88.9% compared to Hou et al. [5], 94.7% compared to Pazouki et al. [17], and 89% compared to Meydani et al. [13].
Emission Costs (\$)	Not explicitly reported	23,317	20,000	18,500	The current work has the lowest emission costs, 7.5% lower than Meydani et al. [13] and 20.6% lower than Pazouki et al. [17].
Total Costs (M\$)	7.48	9.71	6.02	6.64	The current work reduces total costs by 11.2% compared to Hou et al. [5], 31.6% compared to Pazouki et al. [17], while being 10.3% higher than Meydani et al. [13].
REU (%)	99.7	97.0	Not explicitly reported	99.8	The current work achieves the highest REU, slightly outperforming Hou et al. [5] (+0.1%) and significantly outperforming Pazouki et al. [17] (+2.8%).

These studies establish critical groundwork for the optimization of multi-energy systems. Although Hou et al. [5] and Pazouki et al. [17] investigated strategies to improve REU and lower expenditures, their dependence on conventional storage arrangements and elevated EENS metrics highlights deficiencies in both reliability and flexibility. Meydani et al. [13] contributed to the discipline by implementing cost-effective metaheuristic algorithms; however, their methodology did not fully incorporate renewable energy storage systems in a comprehensive manner. This will provide

an almost perfect REU of 99.8%, with an EENS as low as 32 kWh at a total cost of \$6.64M for a robust and scalable solution to sustainable energy systems.

6. Conclusion

This paper proposes an integrated optimization framework for the energy management of multi-energy independent hubs dealing with electricity, thermal energy, and hydrogen systems, considering a set of uncertainties related to the renewable energy sources. The model indeed confirms that

advanced energy management methodologies, including stochastic scenario generation and reduction methodologies, are relevant to counteract the fluctuations of either renewable energy production or consumption. In turn, the suggested approach will ensure that RE sources, CHP units, and hydrogen storage systems are coordinated in an efficient energy dispatch manner, with reduced reliance on non-renewable backups and improved reliability of the whole system. Results demonstrate the flexibility of the system, while the methanation process effectively manages surplus hydrogen and expands energy storage options. The hybrid PSO-GOA optimization algorithm can balance exploration and exploitation of the solution space well and improve convergence in speed and precision. Besides, adding gas

boilers and hydrogen methane conversion can enhance the dynamism while dealing with energy demand. In quantitative terms, it has ensured a renewable energy utilization share of 99.8%, unsupplied energy consumption to 32 kWh, and a total system cost of 3,889.50 \$. Some 65% of the demand for electricity comes from renewables; 85% heat supply is covered by CHP units, supplemented by gas boilers for peak load only. Furthermore, 70% of the hydrogen used will be produced from renewable surplus, 50% of which is subsequently converted to methane for reasons of optimizing storage. These values indicate that this model can be used as one efficient way to find a balance among economic efficiency, renewable energy utilisation, and reliability in the scaling of future energy systems.

Funding

This study was supported by these funding information:

- (1) 2023 Scientific Research Fund Project of the Education Department of Yunnan Province, "Research on Strategies for Improving the moral ability of Yunnan County High School Teachers", Project No. : 2023J1012
- (2.) 2021 Yunnan Philosophy and Social Science Youth Project, Exploration and Research of Yunnan Wetland Ecological Compensation Mechanism based on Water footprint, project number: QN202109
- (3) 2024 Social Science Planning Project of Yunnan Province, Research on Countermeasures of Green Finance to Help Yunnan Agricultural Products Export, Project: SHZK2024314
- (4) 2023 Project of Qujing Social Science Federation of Yunnan Province, Research on the mechanism of digital Finance Driving high-quality development of County economy in Yunnan Province, project number: ZSLH2023ZD01
- (5) Qujing Science and Technology Innovation Joint Special Project: A Comparative study on talent incentive Policies between Yunnan and neighboring provinces (Project No. KJLH2022YB29)
- (6) Scientific Research Fund Project of Education Department of Yunnan Province: Research on Talent incentive Policy in Yunnan under the Background of the Construction of South and Southeast Asia Radiation Center (Project No. 2023J1023)

Reference

1. Ghasemloo A, Kazemi A, Moeini-Aghtaie M. Developing an optimization framework for capacity planning of hydrogen-based residential energy hub. *Int J Hydrogen Energy* 2024;86:185–98. <https://doi.org/10.1016/j.ijhydene.2024.08.378>
2. Eladl AA, El-Afifi MI, Saadawi MM, Siano P, Sedhom BE. Multi-Objective optimal scheduling of energy Hubs, integrating different solar generation technologies considering uncertainty. *International Journal of Electrical Power & Energy Systems* 2024;161:110198.
3. Abedinia O, Ghasemi-Marzbali A, Gouran-Orimi S, Bagheri M. Presence of renewable resources in a smart city for supplying clean and sustainable energy. *Decision making using AI in energy and sustainability: methods and models for policy and practice*, Springer; 2023, p. 233–51. https://doi.org/10.1007/978-3-031-38387-8_14
4. Lin L, Ou K, Lin Q, Xing J, Wang Y-X. Two-stage multi-strategy decision-making framework for capacity configuration optimization of grid-connected PV/battery/hydrogen integrated energy system. *J Energy Storage* 2024;97:112862.
5. Hou H, Liu P, Xiao Z, Deng X, Huang L, Zhang R, et al. Capacity configuration optimization of standalone multi - energy hub considering electricity, heat and hydrogen uncertainty. *Energy Conversion and Economics* 2021;2:122 – 32. <https://doi.org/10.1049/enc2.12028>
6. Oh BC, Son YG, Acquah MA, Kim SY. A new framework for hierarchical multi-objective energy hub planning considering reliability.

Energy 2024;131889.

7. Jia LIU, Zao T, Mojiang YU, Pengzhe REN, Pingliang Z, Wenjie JIA. Robust expansion planning model of integrated energy system with energy hubs integrated. *Electric Power Systems Research* 2024;226:109947.
8. Tiwari S, Singh JG, Garg A. A static robust energy management approach for modelling low emission multi-vectored energy hub including emission markets and power-to-gas units. *Energy* 2024;294:130827.
9. Oyewole OL, Nwulu NI, Okampo EJ. Optimal design of hydrogen-based storage with a hybrid renewable energy system considering economic and environmental uncertainties. *Energy Convers Manag* 2024;300:117991. <https://doi.org/https://doi.org/10.1016/j.enconman.2023.117991>.
10. Shen X, Han Y, Zhu S, Zheng J, Qingsheng LI, Nong J. Comprehensive power-supply planning for active distribution system considering cooling, heating and power load balance. *Journal of Modern Power Systems and Clean Energy* 2015;3:485–93. <https://doi.org/10.1007/s40565-015-0164-5>
11. Luo YH, Liang JL, Yang DS, Zhou BW, Hu B, Yang L. Configuration and operation optimization of electricity-gas-heat energy hub considering reliability. *Automation of Electric Power Systems* 2018;42:47–54.
12. Elkadeem MR, Abd Elaziz M, Ullah Z, Wang S, Sharshir SW. Optimal planning of renewable energy-integrated distribution system considering uncertainties. *IEEE Access* 2019;7:164887–907. <https://doi.org/10.1109/ACCESS.2019.2947308>
13. Meydani A, Shahinzadeh H, Nafisi H, Gharehpetian GB. Optimizing Microgrid Energy Management: Metaheuristic versus Conventional Techniques. 2024 11th Iranian Conference on Renewable Energy and Distribution Generation (ICREDG), vol. 11, IEEE; 2024, p. 1–15. <https://doi.org/10.1109/ICREDG61679.2024.10607783>
14. Alkuhayli A, Dashtdar M, Flah A, El-Bayeh CZ, Blazek V, Prokop L. Designing a multi-objective energy management system in multiple interconnected water and power microgrids based on the MOPSO algorithm. *Heliyon* 2024;10. <https://doi.org/10.1016/j.heliyon.2024.e31280>
15. Soussi A, Zero E, Bozzi A, Sacile R. Enhancing Energy Systems and Rural Communities through a System of Systems Approach: A Comprehensive Review. *Energies (Basel)* 2024;17:4988. <https://doi.org/10.3390/en17194988>
16. Li Z, Xu Y, Fang S, Mazzoni S. Optimal placement of heterogeneous distributed generators in a grid - connected multi - energy microgrid under uncertainties. *IET Renewable Power Generation* 2019;13:2623 – 33. <https://doi.org/10.1049/iet-rpg.2019.0036>
17. Pazouki S, Haghifam M-R. Optimal planning and scheduling of energy hub in presence of wind, storage and demand response under uncertainty. *International Journal of Electrical Power & Energy Systems* 2016;80:219–39. <https://doi.org/10.1016/j.ijepes.2016.01.044>
18. Li Z, Xu Y, Feng X, Wu Q. Optimal stochastic deployment of heterogeneous energy storage in a residential multienergy microgrid with demand-side management. *IEEE Trans Industr Inform* 2020;17:991–1004. <https://doi.org/10.1109/TII.2020.2971227>
19. Zhang X, Conejo AJ. Robust transmission expansion planning representing long-and short-term uncertainty. *IEEE Transactions on Power Systems* 2017;33:1329–38. <https://doi.org/10.1109/TPWRS.2017.2717944>
20. Wang H, Huang J. Joint investment and operation of microgrid. *IEEE Trans Smart Grid* 2015;8:833–45. <https://doi.org/10.1109/TSG.2015.2501818>
21. Yu L, Li YP, Huang GH. Planning municipal-scale mixed energy system for stimulating renewable energy under multiple uncertainties- The City of Qingdao in Shandong Province, China. *Energy* 2019;166:1120–33. <https://doi.org/10.1016/j.energy.2018.10.157>
22. Son YG, Choi S, Aquah MA, Kim SY. Systematic planning of power-to-gas for improving photovoltaic acceptance rate: Application of the potential RES penetration index. *Appl Energy* 2023;349:121611.
23. Qiu R, Zhang H, Wang G, Liang Y, Yan J. Green hydrogen-based energy storage service via power-to-gas technologies integrated with multi-energy microgrid. *Appl Energy* 2023;350:121716.
24. Qiu R, Zhang H, Wang G, Liang Y, Yan J. Green hydrogen-based energy storage service via power-to-gas technologies integrated with multi-energy microgrid. *Appl Energy* 2023;350:121716.
25. Fan J, Zhang J, Yuan L, Yan R, He Y, Zhao W, et al. Deep Low-Carbon Economic Optimization Using CCUS and Two-Stage P2G with Multiple Hydrogen Utilizations for an Integrated Energy System with a High Penetration Level of Renewables. *Sustainability* 2024;16:5722. <https://doi.org/10.3390/su16135722>
26. Luo Z, Dai X, Liu D, Li J, Wang H, Liang J, et al. Bi-level electricity and heat sharing strategy for cross-border integrated energy system

based on Nash game. Appl Therm Eng 2025;258:124704.

27. Pignataro V, Liponi A, Bargiacchi E, Ferrari L. Dynamic model of a power-to-gas system: Role of hydrogen storage and management strategies. Renew Energy 2024;230:120789. <https://doi.org/https://doi.org/10.1016/j.renene.2024.120789>.
28. El-Afifi MI, Sedhom BE, Padmanaban S, Eladl AA. A review of IoT-enabled smart energy hub systems: Rising, applications, challenges, and future prospects. Renewable Energy Focus 2024:100634.
29. Pan G, Gu W, Lu Y, Qiu H, Lu S, Yao S. Optimal planning for electricity-hydrogen integrated energy system considering power to hydrogen and heat and seasonal storage. IEEE Trans Sustain Energy 2020;11:2662–76. <https://doi.org/10.1109/TSTE.2020.2970078>
30. El-Taweel NA, Khani H, Farag HEZ. Hydrogen storage optimal scheduling for fuel supply and capacity-based demand response program under dynamic hydrogen pricing. IEEE Trans Smart Grid 2018;10:4531–42. <https://doi.org/10.1109/TSG.2018.2863247>
31. Li J, Lin J, Zhang H, Song Y, Chen G, Ding L, et al. Optimal investment of electrolyzers and seasonal storages in hydrogen supply chains incorporated with renewable electric networks. IEEE Trans Sustain Energy 2019;11:1773–84. <https://doi.org/10.1109/TSTE.2019.2940604>
32. Deng X, Zhang P, Jin K, He J, Wang X, Wang Y. Probabilistic load flow method considering large-scale wind power integration. Journal of Modern Power Systems and Clean Energy 2019;7:813–25. <https://doi.org/10.1007/s40565-019-0502-0>
33. Yu H, Zhang C, Deng Z, Bian H, Sun C, Jia C. Economic optimization for configuration and sizing of micro integrated energy systems. Journal of Modern Power Systems and Clean Energy 2018;6:330–41. <https://doi.org/10.1007/s40565-017-0291-2>
34. Song X, Liu L, Zhu T, Zhang T, Wu Z. Comparative analysis on operation strategies of CCHP system with cool thermal storage for a data center. Appl Therm Eng 2016;108:680–8. <https://doi.org/10.1016/j.applthermaleng.2016.07.142>
35. Duan J, He Y, Zhu H, Qin G, Wei W. Research progress on performance of fuel cell system utilized in vehicle. Int J Hydrogen Energy 2019;44:5530–7. <https://doi.org/10.1016/j.ijhydene.2018.08.039>
36. Wang Z, Tang Y, Men X. Research on the quantity planning of electric vehicle on the isolated island terminal integration system. Proc CSEE 2019;39:2005–15.
37. Clerc M. Particle Swarm Optimization, vol. 93 John Wiley & Sons 2010.
38. Meraihi Y, Gabis AB, Mirjalili S, Ramdane-Cherif A. Grasshopper optimization algorithm: theory, variants, and applications. Ieee Access 2021;9:50001–24. <https://doi.org/10.1109/ACCESS.2021.3067597>
39. Garg R, Singh AK. Multi-objective workflow grid scheduling using ϵ -fuzzy dominance sort based discrete particle swarm optimization. J Supercomput 2014;68:709–32. <https://doi.org/10.1007/s11227-013-1059-8>

Nomenclature

Nomenclature			
Identifier	Description	Identifier	Description
Abbreviations			
EENS	Expected energy not supplied	PSO	Particle Swarm Optimization
GOA	Grasshopper optimization algorithm	P2G	Power-to-Gas
MEHs	Multi-energy hubs	REU	Renewable Energy Utilization
PDFs	Probability density functions	SOC	States Of Charge
Subscripts and superscripts			
0	Initial	HST	Hydrogen Storage
B	Boiler	IC	Investment cost
CHP	Combined heat and power	i	Index of numbering
Cha	Charge	L	Load
Cap	Capacity	Loss	Not supplied energy
Dis	Discharge	max	Maximum
EH	Energy Hub	MET	Methanation
E	Electric	min	Minimum
EC	Electrolysis cell	OC	Maintenance cost
FCV	Fuel cell vehicles	T	Thermal
fix	Fixed	t	Time
g	Gas	var	Variable

Nomenclature			
Identifier	Description	Identifier	Description
Symbols			
c	Scale parameter	r	Solar radiation
C	Cost	v	Wind speed
H ₂	Hydrogen	w _(s)	Scenarios probability
l	Shape parameter of the Weibull distribution	W	Consumption (required) power
P	Power		
Greek letters			
α, β	Shape parameter of the beta distribution	η	Efficiency
σ	Variance	ε	Limit coefficient
φ	Binary variable that ends the last trip	μ	Mean
ϖ	Hydrogen consumption per mileage		